A STUDY OF INERTIAL FREQUENCY CURRENT OSCILLATION IN THE CENTRAL BASIN OF LAKE ERIE

by
F. M. Boyce, F. Chiocchio

NWRI # 86-201

EXECUTIVE SUMMARY

Circularly polarized, clockwise rotating currents at or near the local inertial frequency are a common occurrence in the offshore regions of the Great Lakes during the stratified season. Often they are the most energetic component of water motion and because they are associated with large vertical shears supported by the stably stratified layers, they may modify, through shear-generated turbulence, the very stratification they depend on. Existing thermocline models used to predict stratification in Lake Erie and elsewhere do not make explicit allowance for this process. This paper focusses on a singlular feature of the Central Basin current records, the occurrence of a marked maximum of inertial frequency motion in July just above the seasonal thermocline. After review of the relevant theory for the generation of inertial frequency motion, the authors propose a simple model that extends Ekman theory to the case of surface wind forcing and subsurface forcing by the pressure gradients (or surface slope) due to wind set-up. Internal wave dynamics are not included. It is found that the subsurface intertial frequency maximum is simulated by a three-layer water column that comprises a wind-stirred upper layer, a bottom layer (hypolimnion) that is stirred by bottom-generated turbulence, and a non-turbulent, stably-stratified metalimnion that is driven primarily by pressure gradients. The model shows that the inertial frequency

response is sensitive to the relative thicknesses of the layers and to the strength and sequence of wind-forcing. Maximum motion occurs when the middle layer is thin, but with increasing shear, the system reverts to two layers. The analysis and model demonstrate the importance of so-called "transient" thermal structure to the dynamics of Lake Erie and underscores the need to make detailed profile measurements of temperature and velocity in the top ten metres of the water column, a zone that has heretofore been seriously undersampled.

RÉSUMÉ À L'INTENTION DE LA DIRECTION

Des courants giratoires en sens horaire, à polarisation circulaire, survenant à la fréquence inertielle locale ou presque, sont un phénomène fréquent dans les zones situées loin des côtes des Grands Lacs en période de stratification. Ils constituent souvent la composante la plus énergétique du mouvement de l'eau et parce qu'ils sont associés à d'importantes forces de cisaillement vertical soutenus par les couches stratifiées stables, ils peuvent modifier, par le biais de la turbulence engendrée par le cisaillement, la stratification même dont ils dépendent. Les modèles de thermocline existants utilisés pour prévoir la stratification dans le lac Érié et ailleurs ne permettent pas de tenir compte explicitement de ce processus. Le présent document porte sur une caractéristique singulière des données sur les courants du Bassin central, à savoir l'existence d'un maximum marqué du mouvement à la fréquence inertielle en juillet juste au-dessus de la thermocline saisonnière. Après avoir examiné la théorie pertinente relative à la production d'un mouvement à la fréquence inertielle, les auteurs proposent un modèle simple qui étend la théorie d'Ekman au cas des forces de vent de surface et des forces de subsurface provenant des gradients de pression (ou pente des surfaces) dus au vent. La dynamique des ondes internes n'est pas incluse. On a constaté que le maximum de la fréquence inertielle de subsurface est représenté par une colonne d'eau de trois couches comprenant une couche supérieure brassée par

le vent, une couche profonde (hypolimnion) qui est brassée par une turbulence engendrée par le fond, et le métalimnion, couche non turbulente à stratification stable conditionnée surtout par des gradients de pression. Le modèle montre que la fréquence inertielle est sensible à l'épaisseur relative des couches ainsi qu'à l'intensité et à la séquence des forces de vent. Le mouvement est maximal lorsque la couche médiane est mince, mais avec une augmentation du cisaillement, le système revient à deux couches. L'analyse et le modèle montrent l'importance de la structure thermique dite "transitoire" pour la dynamique du lac Érié et met en évidence la nécessité d'effectuer des mesures détaillées du profil de la température et de la vitesse dans les dix premiers mètres de la colonne d'eau, zone qui jusqu'ici a été nettement sous-échantillonnée.

A STUDY OF NEAR INERTIAL FREQUENCY CURRENT OSCILLATIONS IN THE CENTRAL BASIN OF LAKE ERIE

INTRODUCTION

Boyce and Chiocchio (1986a) conduct an examination of the gross properties of currents in the Central Basin using spectral and cross-spectral analysis. They show that a salient features of the spectra are large peaks centered on the local inertial frequency (period = 18 hours).Cross-spectral analysis revealed that motions in this band were strongly coherent both horizontally and vertically through the basin. In this paper we examine more closely the spatial and temporal characteristics of these motions and propose a model to explain them.

REVIEW OF THEORY

Before proceeding with an examination of the data, it will be useful to review in brief several theoretical explanations of the ubiquitous clockwise rotating near-inertial motions both above and below the surface in both the open ocean and closed basins.

It has been known for a long time that these motions are intimately connected with the wind and are most vigorous following "favourable" changes in wind speed or direction. In pursuing the link between wind and near-inertial motion, Ekman (1905) laid the foundation for all further study. He argued that a spatially uniform wind blowing over an unbounded ocean should produce the same motion everywhere and consequently horizontal pressure gradients would be unimportant. Wind drag on the water surface would impel the surface water downwind and this moving layer would tend to drag the others along with it due to the presence of turbulence-induced friction, and the flow at all levels would be acted upon by Coriolis force, the steering effect induced by the earth's rotation. The computed response to a suddenly-applied but thereafter steady wind is a steady vertically integrated transport at right angles to the wind direction upon which is superimposed transient circular motions at the local inertial period. The approximate balance of forces in the circular motion is between centrifugal force and Coriolis force. The detailed vertical distribution of mean currents is governed by the distribution of turbulence, parameterized in Ekman's model as a constant eddy viscosity.

Although the concepts of Ekman's (1905) model have been verified time and again, this model does not explicitly recognize the role of the wind as the creator of both the mean current and the turbulence, nor does it recognize the effect of density

stratification. More recent work includes these concepts at the expense of more complex computations. Pollard and Millard (1970), for example, provide a convincing simulation of near-inertial currents in the upper mixed layer (well-mixed turbulent layer adjacent to the surface, at times equivalent to the epilimnion in lakes) with a model that assumes that momentum is transferred very quickly through a mixed layer so that the layer moves as a slab. The strong density gradients at the base of the mixed layer attenuate the vertical component of turbulence and allow the upper mixed layer to slide over the lower layers and consequently, no motion is generated directly in the lower layers. In Pollard's and Millard's model, a damping term is introduced to account for the transient nature of near-inertial motions and in a companion paper by Pollard (1970), it is suggested that some of the energy lost from the mixed layer goes to create near-inertial frequency internal waves. This idea will be discussed more fully below. Pollard's and Millard's model also shows that the near-inertial frequency motions respond not only to the strength of the wind forcing, but also to the particlar sequence of wind events. A wind vector rotating clockwise at the angular frequency of the inertial oscillations will continue to add energy to the motions and increase them, whereas a constant wind or a wind vector rotating in the opposite direction will not remain in phase with the inertial currents.

The basic Ekman dynamics and their modification to suit

the particularities of the upper mixed layer help to explain the presence of near-inertial motions near the surface. The observations show that near-inertial motions are present at all depths, and that they may at times be strongest at mid-depths as opposed to the surface. The density field, which we know to be strongly related to the distribution of turbulence and eddy viscosity, may be implicated directly through the mechanism of internal waves. Starting with the simplest expression of motions in a fluid where the mean density increases with depth (stably stratified), it is possible to show that energy can propagate vertically in the form of plane internal waves. This theory has been successful in accounting for inertial motion at great depths in the ocean (Kundu, 1976, D'Asaro and Perkins, 1984). The group velocity may be expressed in terms of the observed frequency of the near-inertial motion (which the theory shows must always be greater than the local inertial frequency), the local inertial frequency, and the vertical wavenumber of the motion (D'Asaro and Perkins (1984))

$$CG = (SIG*SIG - F*F)/(SIG*BET) \qquad (1)$$

where SIG is the observed angular frequency of the motion, F is the local inertial frequency, and BET is the vertical wave number. When near-inertial motions are well-developed, we observe that SIG is a few percent greater than F. The smallest vertical wavenumber physically realizable is PI/H where H is the total

depth. Taking SIG as 1.05*F and H = 23 m, CG is approximately 7 x 10**-5 m/s; it would take at least 87 hours or 4 inertial periods for the energy to propagate from the surface to the bottom. The signature of such a process in the oceans is the vertical propagation of the phase or direction of the currents. This is detectable in regions of slowly varying density gradients over vertical scales of hundreds of meters. The Lake Erie records show an approximate synchronicity of events at the various levels; nothing what would suggest an accumulation of energy at the bottom delayed by several days with respect to the corresponding surface event. Moreover, during the intervals of significant inertial frequency activity, the phase relations among the various levels remain nearly constant. Indeed the observations suggest a standing wave behaviour in the vertical direction with discrete modes of a structure governed by the density distribution with depth (Royer et al., 1986). How might these be excited?

The classical theory of internal seiches in lakes (Heaps and Ramsbottom, 1966) is an obvious line of enquiry. The simplest expression of this phenomenon occurs in a long narrow lake stratified into two distinct layers by a sharp thermocline. A wind impulse along the lake imparts momentum downwind to the upper mixed layer. The lake boundaries cause an accumulation (downwelling) of epilimnion water on the downwind end of the lake and a loss of epilimnion (upwelling) water from the upwind shore.

Linear theory, applicable to small displacements from the rest state, accounts for the resulting motion as a superposition of the natural modes of oscillation of the basin, both free surface and internal seiches. These seiches may be viewed as trains of opposing progressive waves, the surface seiches associated with trains moving at a speed scaled to the mean depth of the lake , (G*H)**0.5, and the internal seiche, manifested as displacements of the thermocline from the horizontal, associated with wave trains moving at speeds scaled by (G*EPS*H/4)**0.5 where EPS is the relative density difference between the two layers in motion. This theory assumes that both the surface waves and the internal waves are perfectly reflected from the ends of the basin. The extension of this theory to the Central Basin of Lake Erie, requires 1) an examination of the reflection conditions for internal waves when the thermocline intersects a sloping bottom, not a vertical wall, and 2) an extension to include the effects of the earth's rotation.

Munk and Wimbush (1969) provide a simple intuitive criterion for the breaking of gravity waves on a sloping beach. They argue that the acceleration of the wave front up the beach must at all times be less than the component of gravity along the beach in order for the wave to be reflected and not absorbed. For surface waves and other gravitational waves on sharp interfaces, the absorbtion mechanism is wave breaking. When this criterion is extended to near-inertial internal waves of amplitude A on the

interface between two fluids of relative density difference EPS on a beach of slope I with respect to the horizontal, the condition for reflection becomes

$$SIN(I) \;) \; (A*F*F/(G*EPS))**0.5 \qquad (2)$$

where again, F is the local angular inertial frequncy. Taking A as 1 m, EPS as 0.0015, the critical slope I is of the order of .001 or 1 m per km. A cross section of the basin shows that such slopes are attained only within 10 km of the shore on both sides of the basin. Perfect reflection of two-layer inertial frequency internal waves would be assured on both sides of the basin when the main thermocline was less than 10 m deep. Absorbtion of inertial frequency internal wave energy on the south shore of the basin is a distinct possibility during much of the summer.

Assuming for the moment that the lateral boundaries of the basin are prefect reflectors of horizontally-propagating inertial frequency internal waves, we may usefully examine a simple theory by Csanady (1973). This theory is applicable to the generation of internal seiches in long, narrow basins during the early stages of the basin's response to a new wind forcing. Reasoning that the presence of lateral boundaries are felt in mid basin via the propagation of surface and internal gravitational waves, Csanady argues that the effects of the distant ends of the

lake will be felt long after those due to the cross lake motions, and consequently, in the initial phases of the response to a new wind impulse, one may assume constant properties of the motion along the longitudinal axis. This simplification, together with the assumption that one may treat the lake as a two-layer inviscid fluid, reduces the problem to that of a single spatial dimension, the transverse dimension perpendicular to the main axis of the basin. Water is free to move in the longitudinal dimension, and the coupling between longitudinal and transverse motion provided by the Coriolis force ensures that it does so. The problem is further simplified by assuming that the near-inertial motions are manifestations of the internal seiche which may be decoupled from other motions such as the free surface seiche by defining it to have no net transport either along or across the basin. A transport in the upper layer implies an equal but opposite transport in the lower layer. These assumptions reduce the problem to a relatively tractable form, and a further simplification leading to analytical expression of the solution is obtained if one assumes constant total and thermocline depths across the basin. This latter assumption can be shown to have a relatively minor effect, and moreover, it does not obscure the physics of the problem. The solutions for a suddenly applied but thereafter steady wind stress contain a forced, steady portion and an oscillating part. Only the latter is of interest to us. The oscillating part is expressed as the sum of an infinite number of fundamental modes. Expressions for

the oscillating portions of the solution for thermocline displacement and transverse velocity are given below:

```
ETA = 4.*(HB/HT)*TAU/(CI*F)*RB*((F/SIG1)**2*SIN(PI*Y/B)*
      COS(SIG1*T)-(F/SIG3)**2*SIN(3.*PI*Y/B)*COS(SIG3*T)+....)
                                                          (3)

V = 4.*(HB*TAU/HT)/(PI*F)*(-F/SIG1*COS(PI*Y/B)*SIN(SIG1*T)
      +F/(3.*SIG3)*COS(3.*PI*Y/B)*SIN(SIG3*T)-....)       (4)
```

HB is the thickness of the bottom layer; HT is the total depth of the basin. TAU is the wind stress, CI is the phase speed of a long internal wave (CI=(G*EPS*(HT-HB)*HB/HT)**0.5), and F is the local Coriolis parameter (radians per second). RB is the ratio of the Rossby radius of deformation for internal waves, CI/F, to the width of the basin, B. SIG1, SIG3,... are the frequencies of the fundamental modes (see below). Y is the transverse distance measured from mid-basin, and T is the time elapsed from the onset of the wind. Where the ratio RB is small, it can be shown that the thermocline displacements are significant only within a distance R from the shores; elsewhere the modes tend to cancel and the thermocline is flat. Note that only odd-numbered modes are excited by a spatially uniform wind-stress. The frequencies of these modes are given by

$$SIGN = F*(1. + (RB*N*PI)**2)**0.5 \qquad N = 1, 3, 5, \ldots \quad (5)$$

Successive amplitudes of the transverse velocity modes are proportional to

$$AN = F/N*SIGN = 1./N*(1. + (RB*N*PI)**2)**0.5 \quad (6)$$

Successive amplitudes of the thermocline displacements are proportional to

$$ZN = (F/SIGN)**2 = 1./(1. + (PI*N*RB)**2) \quad (7)$$

For the Central Basin of Lake Erie in mid-summer we may take HT = 22m, HB = 5m, EPS = .0015, B = 85 km = 85000 m, F = 1.0 x 10**-4, and G = 9.8 m/s**2. From this we derive CI = 0.23 m/s, a Rossby radius of deformation of 2.4 km, and a ratio RB of 0.028. Frequencies and amplitudes of the first few modes (relative to the first mode) are given in Table 1 which is calculated for a wind stress directed across the lake. The amplitude ratios for a wind stress directed along the lake are multiplied by F/SIGN; there is a more rapid decrease in energy with increasing mode number. For practical purposes, the first and the third modes account for nearly all of the energy in horizontal motions but many modes must be included to represent the thermocline displacements. If this theory is applicable, observed frequencies

in the current meter records should be within a few percent of the local inertial frequency. The presence of significant thermocline displacements associated with the higher modes should shift the spectra of isotherm displacements towards higher frequencies, and one would also expect reduced spatial correlations among these last records because of the presence of many modes of different frequencies. It can be shown that the total currents associated with each mode assume a hodograph in the form of a clockwise rotating ellipse elongated in the longitudinal direction by the ratio F/SIGN.

Csanady's theory, in its simplest, analytical form requires that the lake be of uniform depth, and that both lateral walls be perfectly reflecting to long internal waves near the inertial period. In two layer fluids where one layer is much thinner than the other, the internal wave speed depends primarily on the vertical extent of the thinner layer. This ,of course varies substantially across Lake Erie and would affect the actual modal structures and frequencies. It will be instructive to examine the problem in a different way, to retain time explicitly as an independent variable and to adopt an initial value approach. This has been done by Simons (1978) in an analysis of a similar problem in. Simons' paper studies the generation and propagation of spectacular downwelling fronts on the south shore of Lake Ontario following an isolated but intense wind event

during the International Field Year (1972). The observations consist of a series of repeated temperature cross sections of the lake (Boyce and Mortimer, 1978). Kundu and his colleagues (1983) examine the more complicated problem of a continuously stratified fluid lying beneath an upper mixed layer. Both Kundu and Simons show that the generation of cross-lake internal seiches at near-inertial periods may be viewed as a three-step process. It will be convenient to consider a two-layer fluid of constant depth bounded on the downwind side by a long, straight coastline, the upwind shore of the basin being, in effect, infinitely far away. Imagine that the fluid is initially at rest and is subsequently acted upon by a uniform wind switched on suddenly at T=0 and blowing towards the shore. Away from the shore, the upper layer, acted directly upon by the wind must begin to respond in a fashion similar to that predicted by Pollard (1970), a steady drift of the upper layer at right angles to the wind, and damped, pure, circular inertial motion of the upper layer only. At the coastline itself, motion perpendicular to the shore is prevented; upper layer water impelled by the wind against the shore tends to accumulate there, causing both an elevation of the free surface and a depression of the interface or thermocline. These displacements represent local accumulations of gravitational potential energy which are propagated offshore at the local group velocities for long surface and internal waves. In effect, these waves signal the presence of the downwind shoreline to the offshore region. As mentioned above, the surface gravitational

wave travels at tens of meters per second (G*H)**.5 whereas the internal wave velocity is typically a fraction of a meter per second. The surface gravitational wave conveys to the offshore regions the requirement of zero net flow perpendicular to the coast. Compared to the slower moving internal disturbance, the surface wave displaces but little fluid. The internal wave, moving offshore, accounts for the redistribution of water masses impelled by the winds. This disturbance propagates at the group velocity for long internal waves, unless, as Simons shows, finite amplitude effects intensify the wave into a front moving at up to twice the velocity of a small-amplitude wave. Thus the three-step near-inertial period response at an offshore point: 1) pure inertial motion of the wind-forced layer until the arrival of the surface gravity wave from the shore (about 1 hour in Lake Erie), 2) inertial motion in both layers, but in opposite directions until the arrival of the internal wave front (about 40 hours in Lake Erie), 3) inertial-gravitational motions at frequencies higher than inertial (internal seiches in basins of finite width and reflecting shorelines). In basins of finite width, regime 1) is of short duration and for this reason, many analysts prefer to simplify the problem by assuming that the surface wave propagates infinitely fast, or what is equivalent, that the upper bounding surface of the fluid is a frictionless rigid lid. Almost immediately after the onset of a wind one expects to see inertial period motion through the water column, primarily wind-forced in the upper layer, pressure-gradient driven beneath the surface.

The division between flow and counterflow in the fluid seems to depends on the stratification of the water column. Regime 2), the interval between the arrival of the surface gravity wave and the internal wave front lasts approximately 37 hours or two inertial periods in the middle of the Central Basin. Assuming no other source of gravitational potential energy, we would expect that after this time the frequencies of the near-intertial motion to increase sightly. Another source of gravitational potential energy is the interaction of the initally pure inertial flow with variable bottom topography. The bottom of the Central Basin of Lake Erie has little relief to be sure, but it is not totally flat. The mixture of "pure" inertial motion and inertial-gravitational waves might be expected to produce a groupiness of the near-inertial signal, the modulating frequency being a difference between the pure inertial frequency and the inertial-gravitational frequency (a few percent above F). This mechanism should produce packets of up to 10 cycles. Kundu (1984) has extended his earlier analysis to include the effects of varying winds and shows that randomly varying winds can produce larger inertial period motions than step wind inputs but that these motions are intermittent in time and less coherent in the vertical dimension. With this theoretical overview, we now turn to a more detailed analysis of currents and temperatures near the inertial period in the Central Basin of Lake Erie.

erie5b.mai 29/07/86

PRESENTATION OF DATA

Distribution of inertial frequency and fundamental seiche frequency motions in time.

Inertial frequency motion and fundamental seiche frequency motion are readily detected in the spectra of currents and temperatures, but their presence is episodic and analysis in the time-domain is also required. The main tool used for this purpose is complex demodulation (Bloomfield, 1976, Boyce, 1986). Suppose that a time series contains a significant term of the form A(T)*COS(WO*T + PHI(T)) where A(T) and PHI(T) are are an amplitude and a phase angle that vary significantly at frequencies much less than WO. Using numerical techniques analogous to the detection of the audio signal on an amplitude-modulated radio frequency, it is possible to compute a running, time-averaged estimate of A(T) and PHI(T). These may be used to reconstitute an estimate of the original signal, in which case the technique works as a narrow band-pass filter, or the estimates of A(T) and PHI(T) for each component of a horizontal current may be used to construct a time-varying hodograph of the currents at the central frequency, WO. The penalty paid for a narrow resolution in frequency is the necessity to average over

long periods of time, smoothing or smearing the signal. If the signal frequency is constant, close to but not exactly WO, then the function PHI(T) will show a steady increase or decrease. The time-derivative of PHI(T) may be viewed as a frequency correction, yielding a better estimate of WO. This last calculation is valid only if the signal frequency constitutes an isolated peak in the total spectrum.

Figure 1 is derived from two complex demodulations of the 10 m current vector at station 29 (41 51.8'N by 81 54.8'W) in the mid-basin array from June 11 to September 17, 1979. The central frequencies are .0558 cph (inertial frequency) for the first pass, and 0.0690 (fundamental seiche frequency) for the second. The nominal bandwidth of the calculation is +/- 0.01 cph. In this representation, the extracted signal is expressed as a compressed hodograph and the figure shows the lengths of the major and minor half-axes of the current ellipse plus the direction of rotation. Orientation of the ellipse and phase information can be extracted from the computations but are not presented in this diagram. A stick vector plot of low-pass filtered winds is included. From mid-June to mid-July a clockwise rotating inertial period component is present, having a typical amplitude of 5 cm/s. Most of the time the motion is almost circular, with the major and minor axes of the current ellipse of nearly equal length. Motion detected at the fundamental seiche period is more variable and much less energetic. The stronger episodes show a marked elongation of the current ellipse,

approaching rectilinear motion. The direction of rotation of the current vector may be positive or negative. The mid-July to mid-August record (Figure 1b) is remarkable for the large motions (both frequencies) observed in the last days of July and the first few days of August. The vector plot of the winds shows two episodes in this interval where the wind vector rotates rapidly in a clockwise direction through almost a full 360 degrees, a condition favouring a transfer of energy to the inertial period water movements. During the mid-August to mid-September period, despite stronger winds, inertial frequency components are weak, becoming confused by the end of the period. The fundamental seiche motion is more variable in time but retains its rectilinear form.

Figure 2 brings together the wind data, the thermal structure (isotherm plots from station T45 in the middle of the array) and the compressed hodograph version of the 10 m inertial frequency currents for the period of enhanced inertial frequency motion centred on August 1, 1979. The thermal structure panel shows an evolution from mid-July to mid August from a broad thermocline region, with stratification at times extending to the surface, to a very sharp thermocline, effectively a two-layer structure. At the time of maximum inertial frequency motion, the water column has three distinct layers, a well-mixed upper layer, a thermocline region with strong density gradients, and a well-mixed bottom layer.

Figure 3 provides another view of the same episode. The cross lake component of current is plotted at three depths, 10, 15, and 19m from July 24 to August 20, 1979. The figures show both the hourly-averaged data and the reconstructed component from the complex demodulation analysis. The most cursory glance at the figure shows that the episode shifts between two distinct regimes on August 9. July 24 to August 9 contains the largest observed inertial frequency motions. These are at once obvious in the raw data; the reconstructed, notch-filtered signal tracks the phase of the raw data quite well, but fails to follow some of the more abrupt changes in amplitude. The enhancement of the oscillations at the 15 m depth is clear. The phase relationship among the three measurements is such that the 15 m and the 19 m oscillations are in phase with one another, but in opposition (180 degrees) to the 10m measurement. From Figure 2 it is seen that the 10 m current meter lies in the upper mixed layer, the 19 m instrument is in the bottom mixed layer, while the 15 m instrument is in the thermocline region during the July 24 to August 9 period. The second half of the record is distinguished by the reduction in amplitude of the inertial frequency oscillations in the 10 and 15 m record and by the increased high-frequency content of the records at all levels, but especially in the 15 and 19 m levels. The most probable source of high frequency energy in the records are orbital motions from surface waves that accompany the strong winds of this period.

These motions tend to be filtered in the 10 m record because of the particular design of the current meter (Plessey MO21) whereas the 15 m and 19 m instruments have savonius rortors (Geodyne), known to rectify oscillating motion. The "noise" amplitude on the 19 m record is about half that of the 15 m record. For example, a 1.5 m crest-to-trough wave on 23 m of water and with a period of 4 seconds produces maximum orbital wave speeds of 5 cm/s at 15 m and 2 cm/s at 19 m, roughly consistent with the observations. The phase relationship of the inertial frequency components has changed. In this interval the 10 m currents are in opposition to the 19 m currents, as before, but the 15 m currents are in phase with the 10 m currents, where formerly they were in opposition. As the thermocline layer becomes thin and the thermocline deepens, the 15 m current meter finds itself in the upper mixed layer. The increased thickness of the upper mixed layer also accounts for its reduced velocities.

Distribution of inertial frequency fluctuations of velocity and temperature in space.

Figure 4 is derived from the complex demodulation of all the available current meter records in the cross-lake transect. The amplitude, phase, and frequency of the inertial frequency component is extracted for the time 0000h Z, July 30, 1979, during the interval of maximum inertial frequency motion. These values are laid out on a plot of the lake's cross section. Phase

angles are referred to the 10 m level at station 27. Generally speaking, the portion of the section north of but including Station 27 conforms to the pattern of Figure 3 during the interval of maximum inertial frequency motions. Station 34, to the south of Station 27, shows surface and bottom currents to be out of phase with each other but as much as 50 degrees out of phase with Station 27. The phase at the other two stations near the south shore is variable. This pattern is repeated through the interval of largest inertial frequency motions.

With the same organization of Figure 3, Figure 5 now shows the vertical displacements of the 16 C isothermal surface at each of the mid basin thermistor arrays. Excursions of this surface from its mean depth are of the order of 1 m. Amplitudes of the filtered inertial frequency signals are smaller and vary from site to site. The motion is approximately in phase across the array during the largest inertial-frequency oscillations around August 1, 1979. At Station T45, located close to the central Station 27, there are significant higher frequency oscillations at periods close to 8 hours. These are much less pronounced at the other stations. Other lower frequency motions are also approximately in phase. The phase relationship between the currents and the vertical displacement during the large motions is such that maximumn upward displacement, leads maximum southward 10 m cross-lake current by 90 degrees, that of a standing wave. This analysis is extended both north and south of

the mid-basin array by correlating the temperature fluctuations recorded at the 15 m current meters with the currents themselves. A phase relationship between the cross-lake component of current and the temperature, consistent with the isotherm displacements is obtained locally from Station 9 south to Station 35, more than two-thirds of the distance across the basin, although as Figure 4 shows, the phase with respect to the central station varies. If one were dealing with a transverse first mode internal seiche, then one should expect a nodal point in the thermocline displacement somewhere in mid-lake and a shift by 180 degrees of the phase relationship. No consistent phase relationship is obtained between the temperature and the along-lake component of current. It is unclear from the measurements how the flow adjusts to the presence of the shoreline although the limited observations are consistent with the idea that the gently sloping sides of the basin at the depth of thermocline contact are poor reflectors of inertial frequency motion and hence that well-defined standing inertial-gravitational waves are absent.

lay3.mod 06/08/86

A SIMPLE THREE-LAYER MODEL OF INERTIAL FREQUENCY CURRENTS IN THE CENTRAL BASIN OF LAKE ERIE

In a previous paper (Boyce and Chiocchio, 1986, this volume) it was pointed out that the bottom currents in mid-basin sometims behaved as if they were driven by a force directed opposite to the surface wind stress, while the 10 m currents, part of the surface mixed layer, responded to the wind stress directly. We also note once again the occasions when the inertial frequency currents at 15 m depth are larger than those above or below. A simple three-layer model simulates these effects.

The basic hypothesis we propose is that the generating mechanism for inertial frequency currents in the Central Basin of Lake Erie is that described by Kundu et al (1983) and reviewed earlier, where the presence of the lateral boundaries of the basin is felt in mid-basin as a pressure gradient but otherwise the flow is described by Ekman dynamics. The vertical distribution of velocity is influenced by the density field only insofar as this distribution affects the vertical distribution of stress through the fluid. This theory may not be valid for times beyond that required for a long, large amplitude internal wave to propagate from the shoreline to the middle of the lake, but because the wind field varies significantly over time intervals

shorter than this, the theory may be adequate for describing the continuing adjustments of the velocity field. Furthermore, Boyce and Chiocchio (1986) show that the flow depends only weakly on the internal pressure gradients. We seek the simplest possible model capable of expressing this hypothesis, and in so doing we make the following assumptions:

1) The flow comprises three layers. Within each layer the horizontal velocities are uniform, both vertically and horizontally. The layers are separated by interfaces that may move vertically as fluid is entrained from a non-turbulent layer into a turbulent layer.

2) The top layer is acted on by wind stress and the bottom layer is acted on by friction as it moves over the bottom. These stresses maintain the layers in a state of turbulence sufficient to ensure a uniform vertical distribution of mean momentum through the layers; the mean motion of each layer is that of a slab. Both turbulent layers may entrain water and mean momentum from the non-turbulent middle layer; the entrainment of momentum results in forces exerted on the entraining layers. Velocity shears between the layers may also be reduced through interfacial friction. In our simplified "slab" model, both the entrainment "stress" and the interfacial friction enter the equations of motion in the same way with the exception that the effective friction coefficient due to entrainment varies with time.

Although we show both terms in the equations, we simplifiy the model by retaining constant friction coefficients throughout, chosen so as to represent the average damping. All layers are acted on uniformly by an external surface pressure gradient.

3) The surface pressure gradient is the result of the accumulation of water against the shore of the lake (setup) in response to wind forcing. It is transmitted to mid lake via long surface gravity waves. The setup time in Lake Erie is short compared with the inertial period. Thus we choose to neglect the propagation time of surface waves and assume that the surface setup that nullifies net transport takes place instantaneously. The mathematical expression of this assumption is a condition of zero vertically integrated transport holding at all times.

In the notation we have chosen, the subscript 1 refers to the top or surface layer, the subscript 2 refers to the middle layer, and the subsript 3 to the bottom layer. The symbol u refers to the component of velocity (positive eastward) along the major axis of the basin. v refers to the component of velocity (positive northward) perpendicular to the major axis. H refers to the layer thickness. The equations of motion for flow parallel to the major axis of the basin are written:

$$\frac{du_1}{dt} - fv_1 = \frac{1}{H_1}\frac{dH_1}{dt}(u_2-u_1) + \frac{w_1}{H_1}(v_2-u_1) + \frac{F_1}{H_1} - \frac{\partial \varphi}{\partial x} \quad (8)$$

$$\frac{du_2}{dt} - fv_2 = -\frac{w_1}{H_2}(v_2 - u_1) - \frac{w_3}{H_2}(v_2 - u_3) - \frac{\partial \varphi}{\partial x} \qquad (9)$$

$$\frac{dv_3}{dt} - fv_3 = \frac{1}{H_3}\frac{dH_3}{dt}(v_2 - v_3) + \frac{w_3}{H_3}(v_2 - v_3) + \frac{F_3}{H_3} - \frac{\partial \varphi}{\partial x} \qquad (10)$$

The zero net transport condition is written:

$$v_1 H_1 + v_2 H_2 + v_3 H_3 = V_1 H_1 + V_2 H_2 + V_3 H_3 = 0 \qquad (11)$$

The "rigid lid" condition is also required:

$$H_1 + H_2 + H_3 = H_T = \text{constant} \qquad (12)$$

From these five equations, the x-component of the pressure gradient may be expressed in terms of the surface and bottom stresses:

$$\frac{\partial \varphi}{\partial x} = \frac{F_1 + F_3}{H_T} \qquad (13)$$

A similar expression obtains for the y-component of the pressure gradient. Using equation 13 and 11, the six equations of motion reduce to four independent equations which we choose to express

the motion in the top two layers:

$$\frac{du_1}{dt} - fv_1 = -k_{11}u_1 - k_{12}v_2 + P_1 \qquad (14)$$

$$\frac{dv_1}{dt} + fu_1 = -k_{11}v_1 - k_{12}v_2 + Q_1 \qquad (15)$$

$$\frac{du_2}{dt} - fv_2 = -k_{21}u_1 - k_{22}u_2 + P_2 \qquad (16)$$

$$\frac{dv_2}{dt} + fu_2 = -k_{21}v_1 - k_{22}v_2 + Q_2 \qquad (17)$$

The coefficients $k_{11}, k_{12}, k_{21}, k_{22}$ and the terms P_1, P_2, Q_1, Q_2 are defined in Table 2. The bottom stress has been expressed as a linear function of velocity in the bottom layer:

$$F_3 = -w_B u_3 \quad , G_3 = -w_B v_3 \qquad (18)$$

Analytical expressions for constant layer depths and idealized wind forcing are simply obtained by Laplace Transform methods. We present solutions below of the cross-channel components of velocity for a simple case in which the wind stress is a step function applied along the major axis of the the lake at t = 0. The layer thicknesses remain constant, interfacial friction is set to zero, but bottom stress is retained.

$$V_1(t) = \frac{-F_1}{f}\left\{1-\left[\frac{H_2 H_T}{(H_T-H_1)(H_T-H_3)} + \frac{H_3 H_1}{(H_T-H_1)(H_T-H_3)} e^{-\Omega t}\right]\cos ft\right\} \quad (19)$$

$$V_2(t) = \frac{-F_2}{f}\left\{1-\left[\frac{H_T}{(H_T-H_3)} - \frac{H_3 e^{-\Omega t}}{(H_T-H_3)}\right]\cos ft\right\} \quad (20)$$

$$V_3(t) = \frac{-F_2}{f}\left\{1 - e^{-\Omega t}\cos ft\right\}$$

$$\Omega = \frac{\omega_B}{H_T}\left(\frac{H_T}{H_3} - 1\right)$$

The structure of equations 19 and 20 are the same; the steady component is balanced initially by the oscillating component. When H1 and H2 are unequal, the amplitude of the oscillating component may grow with time before decreasing. Figure 616 the response of the model two a "top hat" wind stress of varying duration when the layer depths are held constant. The complete solution is the sum of two modes of oscillation. A frictionally damped mode is found in all three layers; its net transport must sum to zero. An undamped, pure inertial mode is confined to the upper two layers. It too must integrate across the upper two layers to yield zero transport. The amplitudes are in inverse proportion to the layer thicknesses; thus when the middle layer is thin, velocities in it will be large. Motion in the middle and bottom layer always oppose motion in the surface layer. As the middle layer becomes thin, its velocity increases; the fastest inertial period currents may occur in the middle layer. This is exactly what we observe; the largest inertial period motions occur in the layer between the actively mixed upper layer and the seasonal thermocline at times when this layer is sufficiently thick; they are out of phase with the motions in the surface (wind-driven) layer but in phase with the motions in the bottom

layer. Note that as the wind-mixed layer becomes thicker at the expense of the middle layer, the amplification factor between the magnitude of the velocity in the middle layer and the velocity in the upper layer becomes larger. The velocity shear between the upper and the middle layer (larger than the shear between the middle and the bottom layer because of the phase relationships and taking place in a zone of relatively weak density gradients) may become a significant source of turbulence and mixing leading to the incorporation of the middle layer into the upper layer.

The winds being variable, the data contain few, if any events where the theory could be tested simply and quantitatively with analytical solutions of the velocity field. We have coded equations 15 through 17 numerically. Inputs to the computation are estimates of wind stress formed from meteorological observations at Station 24 (to the north of the main array - the record at Station 27 is incomplete), and the layer thickness, derived from the thermistor array at Station 27. These are established simply by estimating the level at which the temperature departs significantly from the mixed layer temperature, starting from the top and from the bottom. Because of the high-frequency variability in the thermistor array data, the layer thicknesses are smoothed with a low-pass filter before running the model. Note that not only do the layer thicknesses enter the calculations directly as coefficients, but also the time derivatives of the layer thickness appear as time-varying

damping factors. These we consider to be effective only during periods of actual entrainment and thickening of the turbulent layers. The upper mixed layer may reform each day; the smoothed estimates of layer thickness show intervals when the mixed layers are becoming thinner. During these intervals we would assume that the entrainment-damping was zero. Aiming for the utmost simplicity, however, we neglect the time-varying damping, and express all internal loss terms as interfacial friction, choosing constant friction coefficients that give the best fit of model to observations. The middle layer, as defined, may become very thin and the three layer model can assign unrealistically high velocities to it. To avoid the extra complication of incorporating a model of shear-induced mixing, we have arbitrarily set a minimum thickness of the middle layer required for a three-layer model. When the middle layer thickness is less than this limit, we switch over to a dynamically similar two-layer model in which the middle layer and the bottom layer are included together as the new bottom layer.

We have chosen to simulate the periods from July 23 to August 15, 1979 and from August 1 to 31, 1980. The first period is of particular interest because the stratification progresses from a three-layer to a two layer situation during the strong winds of early August, a transition period that includes the largest observed inertial period currents at the 15 m depth. This is the same period simulated by Ivey and Patterson, 1984. The

1980 period includes the anchor station period and the GVAPS experiment described by Royer et al. (1986b) in this volume.

Figure 7 shows the observed cross-lake component of velocity at three depths (10, 15, and 19 m) at Station 27, the wind stress amplitude (taken as proportional to the square of the wind velocity), and the observed depths of the interfaces between the layers. These were computed as the depths at which the water temperature differed from the surface or bottom temperature by more than 0.75 C. Smoothed values of wind stress and layer depth are presented in the figure. Smoothed values of layer depth were introduced to the model, but unsmoothed, hourly values of wind stress were input. The model output is plotted as a dashed line on the same time axis as the current meter most representative of that layer. The model was run many times with different values of wind drag coefficient, bottom and interfacial friction timescales. The results presented are judged to be close to optimum. We found, in particular, that interfacial friction was an essential ingredient and that the friction coefficient or timescale had to be similar for both interfaces in order to maintain the "correct" phase relationship between layers.

With regard to Figure 7, the model shows uneven results prior to the major input on August 2. Strong inertial frequency oscillations are observed at 15 m starting 28 July, and indeed thw wind record presented in Figure 1 shows this to be one of

the episodes of clockswise rotating winds that are known to encourage the growth of inertial oscillations. The model fails to simulate these oscillations but the response to the strong winds of August 2 is convincing in all three layers, in both the three-layer and the two-layer versions. To interpret the record one must be aware of the fixed point currents meter's position relative to the mean depth of the interfaces. For example, during the two layer part of the fun, the 15m current meter lies close to the upper surface of the thermocline where it experiences a transition regime.

Figure 8 is identical to Figure 7 except that the simulation is performed over the interval 19 August to 9 September, 1979. Following the strong winds in mid-August that collapse the thermocline layer into a narrow region of strong gradients, and the basin into an effective two-layer system, solar heating forms a shallower upper mixed layer and the basin returns briefly to a three-layer system. On 22 August (see Figure 1c) the wind vector rotates in the clockwise dierection favourable to the creation of intertial frequency motions. The 19 m observed currents respond strongly with a train of inertial frequency oscillations. The model output that best simulates this motion is from the middle layer. This is because the 19 metre instrument is now positioned above the main thermocline.

Figure 9 is again identical to Figure 7 except that the

simulation is performed using August, 1980 data. Once again, the model simulated the enhanced inertial period oscillations near mid-month.

It is puzzling that the model should simulate some of the observed inertial frequency bursts but not others. The wind episode of July 26 - 27 where the winds rotate in a clockwise direction is obviously favourable for the creation of positively rotating surface currents. The model predicts currents that are out of phase with the observed currents and much smaller. A rerun of the computations starting at July 26 and eliminating earlier motions showed that initial conditions were not responsible. A glance at the FTP records for this episode suggests that motions at frequencies higher than inertial may be present at that time; the wind impulse may have triggered a response that included gravitational components, something that the model is unable to simulate. It should also be noted that the wind record used as input to the model is from Station 24 well to the north of the main array and may differ at crucial times from the actual wind stress applied to Station 27.

CONCLUSIONS

This paper has two main thrusts. The first is to examine the prominient inertial frequency oscillations in terms of the several possible theoretical explanations, and the second is to demonstrate the intimate coupling between the horizontal velocity field and the vertical thermal sturcture that must be accounted for in a realistic modelling scheme.

Boyce and Chiocchio (1986, this volume) point out that the bottom currents in the Central Basin often behave as if they were driven by a force opposed to the local wind stress. This is consistent with the setup or tilt of the lake's free surface in response to wind being accomplished in a time short compared with the local inertial period. In mid-basin, this effect is modelled by constraining the vertically integrated transport to be zero at all times.

Another finding (Boyce and Chiocchio, 1986) discussed previously and in this paper, is that internal pressure gradients and their manifestations such as vertical isotherm dislacements are poorly correlated over length scales of 10 km or more, whereas the horizontal velocity field, near the inertial frequency is strongly coherent over tens of km.

Csanady's (1973) study of transverse internal seiches in a long lake assumes that the baroclinic component of flow can be explained in terms of a superposition of transverse internal seiches, the natural modes of the basin, assuming that the boundaries of the lake are perfect reflectors of wave energy. This theory predicts that the thermocline displacements necessary to accomodate baroclinic flow in a closed basin are confined to within one Rossby radius of deformation of the shoreline (nominally 2 - 3 km). Csanady's theory is supported by the observation that the major bursts of near-inertial frequency motion have frequencies a few percent greater than the local inertial frequency. No evidence is provided for enhanced vertical displacements of the isotherms near shore that are coherent with the inertial frequency currents; analysis of temperatures and currents measured together do not support a standing wave interpretation; simple theory suggests that the basin boundaries may not reflect inertial frequency internal waves. This theory cannot properly account for the initial build-up of motion in the basin.

The initial value problem posed by Kundu is more realistic and allows for the propagation of boundary effects into mid-basin at the appropriate wave speed. The zero transport condition is equivalent to the assumption that the surface gravitational waves move so fast relative to the other scales of motion that their propagation times can be ignored. Immediately

following a wind impulse pure inertial motion should appear throughout the water column, the motion at depth being oppositely directed to that in the wind-driven layer, until such time as internal waves propagate out from the shore or are generated locally by the bottom topography. Possibly because of the variable wind-forcing, a clear trace of this process does not appear in the data; the phase of the notch-filtered signal is subject to sudden variations.

In order to account for the observed maximum of inertial frequency oscillations at the 15 m depth (above the main thermocline) it is necessary to invoke the presence of three moving layers, Adjacent to the bottom and the surface are two mixed layers, the top one driven directly by the wind, and the second, or bottom layer, while powered by the surface pressure gradient or wind set-up, is mixed by the turbulence generated by flow over the bottom. The middle layer is one of stable stratification that forms under calm heating conditions. Its thickness is highly variable. The middle layer responds to the surface pressure gradients alone, with the exception of relatively small stresses generated at the sheared interfaces. A very simple model of this system, one that neglects the gravitational component, shows that there are two modes of inertial oscillation: a damped mode present in all layers that removes the energy lost in doing work against bottom friction, and an undamped, pure inertial mode, shared only between the top

and middle layers. An analysis of the vertical profiler records (GVAPS) made in 1980 shows a similar modal structure (Royer et al, 1986b). The transports in each mode sum independently to zero, and for a step input, the initial sum of both modes is to zero velocity in all layers. When the middle layer is thin relative to the top layer, its second-mode velocities are augmented, and it is this effect that produces the large inertial-frequency oscillations in the middle layer.

Using measured winds and temperature profiles as input, the model simulates the important features of the observed intertial frequency oscillations. In particular, it demonstrates the sensitivity of the system to wind input. More important than the amplitude of the stress is the rate of change of wind direction; all of the major bursts of inertial frequency energy are associated with clockwise rotating wind vectors. When the middle layer becomes thin enough, the two shear zones coalsece into one and the system reverts to two layers. In this configuration, there is only one shear mode possible, the one corresponding to damped motion. Consequently, the inertial frequency "ringing" available to the three-layer system is absent and the system is visibly less resonant. The model is unable to simulate the inertial gravitational modes and the consequent increase in frequency. However the durations of the inertial frequency bursts are short enough in practice that the model remains effectively in phase with the observations.

The model has served its purpose as a dignostic tool and is too crude a vehicle for accurate predictions. However, a combination of the present simulation of the mean motion toether with a turbulent energy budget approach to the development and decay of the mixed layers (buoyancy and mixing) would be a challenging followup to this study and would possibly lead to improved modelling of the Central Basin temperature and velocity structure.

The study underlines the importance of the "transient" thermal structure in controlling the distribution of horizontal velocity and presumably, other parameters of biochemical importance in the Lake Erie water column.

REFERENCES

Bloomfield, P. 1976. Fourier analysis of time series: an introduction. John Wiley and Sons, Inc. New York.

Boyce, F.M. and C.H. Mortimer, 1977. IFYGL temperature transects, Lake Ontario, 1972. Technical Bulletin No. 100, Canada Centre for Inland Waters, Burlington, Ontario, 315pp.

Boyce, F.M. 1986. Complex demodulation routines for current meter time-series. NWRI contribution 86-**.

Boyce, F.M. and F. Chiocchio, 1986. Time and space scales of motion at a mid-Central Basin site. J. Great Lakes Res. XX: yyy-zzz.

Csanady, G.T., 1973. Transverse internal seiches in large oblong lakes and marginal seas. J. Phys. Oceanogr. 3: 439-447.

D'Asaro, E.A. and H. Perkins, 1984. A near-inertial internal wave spectrum for the Sargasso Sea in Lake Summer. J. Phys. Oceanogr. 14: 489-505.

Ekman, V.W., 1905. On the influence of the earth's rotation on ocean currents. Ark. Mat. Astron. Fys. 2(11): 52p.

Heaps, N.S. and A.E. Ramsbottom, 1966. Wind effects on the water in a narrow two-layered lake. Phil. Trans Roy. Soc. London, 259 A. 1102: 391-430.

Ivey, G.N. and J.C. Patterson, 1984. A model of the vertical mixing in Lake Erie in summer. J. Limnol. and Oceanogr. 29: 553-563.

Kundu, P.K., 1976. An analysis of inertial oscillation observed near the Oregon Coast. J. Phys. Oceanogr. 6: 879-892.

Kundu, P.K., Chao, S.-Y., and J.P. McCreary, 1983. Transient Coastal Currents and inertio-gravity waves. Deep-Sea Research 30: 1059-1082.

Kundu, P.K., 1984. Generation of Coastal inertial oscillations by time-varying wind. J. Phys. Oceanogr. 14: 1901-1913.

Munk, W. and M. Wimbush, 1969. A rule of thumb for wave breaking over sloping beaches. Soviet Oceanology 9: 56-59.

Pollard, R.T., 1970. On the generation by winds of inertial waves in the ocean. Deep Sea Research 17: 795-812.

Pollard, R.T. and R.C. Millard Jr., 1970. Comparison between observed and simulated wind-generated inertial oscillations. Deep

Sea Research 17: 813-822.

Royer, L., Hamblin, P.F., and F.M. Boyce, 1986. A comparison of drogues, current meters, winds, and a vertical profiler in Lake Erie. J. Great Lakes Res. XX: yyy-zzz.

Royer, L., Hamblin, P.F., and F.M. Boyce, 1986. Analysis of continuous vertical current profiles in Lake Erie. Atmosphere-Ocean 24: 73-89.

Simons, T.J. 1978. Generation and propagation of downwelling fronts. J. Phys. Oceanogr. 8: 571-581.

TABLE CAPTIONS

Table 1. Mode number, frequency relative to the local inertial frequency, period (hours), amplitude of the transverse velocity relative to that of the first mode, amplitude of thermocline displacement relative to the first mode displacement for transverse seiches excited by a cross-lake wind (step input) based on a theory by Csanady (1973). Parameters are chosen to fit the Central Basin of Lake Erie: Total depth (HT) = 22m, Hypolimnion thickness (HB) = 5m, coriolis parameter (F) = 0.0001, cross-lake dimension (B) = 85 km, density contrast (EPS) = 0.0015, internal wave speed (CI) = 0.23 m/s, internal Rossby radius of deformation (RI) = 2.4 km.

Table 2. Definition of coefficients in model equations. k = bottom friction parameter (1/timescale), dH1/dt = downward velocity of interface between upper mixed layer and thermocline, dH3/dt = upward velocity of interface between lower mixed layer and thermocline. W1 is friction parameter for the top interface, W3 for the bottom. F1 is the along lake component of wind stress, and G1 is the across-lake component (both divided by density).

Table 1.

N	SIGN/F	PERIOD(HRS)	AN/A1	ZN/Z1
1	1.0039	17.8	1.000	1.000
3	1.0348	17.3	0.323	0.941
5	1.0939	16.4	0.183	0.841
7	1.1771	15.2	0.122	0.726
9	1.2796	14.0	0.087	0.614

Table 2.

$$k_{11} = \frac{1}{H_1}\left(w_1 + \frac{dH_1}{dt}\right) + w_B H_1 / H_3 H_T$$

$$k_{12} = -\frac{1}{H_1}\left(w_1 + \frac{dH_1}{dt}\right) + w_B H_2 / H_3 H_T$$

$$k_{21} = \frac{H_1}{H_3}\left(w_B / H_T + \frac{1}{H_2}\left(w_3 + \frac{dH_3}{dt}\right)\right)$$

$$k_{22} = \left(\frac{H_2 + H_3}{H_2 H_3}\right)\left(w_3 + \frac{dH_3}{dt}\right) + \frac{H_2 w_B}{H_3 H_T}$$

$$P_1 = F_1\left(\frac{H_T - H_1}{H_1 H_T}\right) \qquad P_2 = -F_1 / H_T$$

$$Q_1 = G_1\left(\frac{H_T - H_1}{H_1 H_T}\right) \qquad Q_2 = -G_1 / H_T$$

FIGURE CAPTIONS.

Figure 1. Six-houly stick vector plot of smoothed wind speed (Station M24), compressed representation of current ellipses derived from complex demodulation of the 10 m currents from Station 29 at two frequencies (0.0558 cph, the local inertial frequency, and 0.0690 cph, the first mode free surface seiche). The figure consists of three panels, (a), (b), and (c) ranging from June 11 to September 17, 1979. The ellipse is represented by maximum and minimum speeds (major and minor half axes). The maximum speed is indicated by a straight line drawn vertically from the time axis. The minimum speed is marked on that line by a triangle, formina an arrow. An upwards pointing arrow indicates positive, clockwise rotation of the current vector, a downward pointing arrow indicates negative, counter-clockwise rotation of the vector.

Figure 2. The top two panels of Figure 1(b) (wind and current ellipse for motions near the local inertial frequency) are combined with a plot of isotherm depths from Station T45 (near Station 27 in mid-array) to show the influence of wind and thermal structure on inertial frequency oscillations.

Figure 3. Cross lake component of velocity at three levels, 10, 15, and 19 m at Station 27 from July 24 through August 20, 1979. This figure shows both houly averaged current meter data (spiky) and the output of a notch filter (smooth) of total bandwidth 0.02 cph centred on the local inertial frequency (0.0558 cph). The filtered signal is derived by complex demodulation. Other products of this technique used in Figure 4 are the orientation of the current ellipse and the phase of the vector.

Figure 4. Cross section of Lake Erie's Central Basin running through the main array showing current amplitudes, phases, frrequency difference with respect to the local inertial frequency, and temperature, for the complex demodulated signal centred on the local inertial frequency, 0000 GMT, July 30, 1979.

Figure 5. Figure of construction very similar to Figure 3 showing the displacement of the 16 degree isothermal surface at the three thermistor array locations in mid basin. The notch filtered signal centred on the local inertial frequency is superimposed.

Figure 6. Response of numerical model compared with approximate analytical solutions of equations 14 through 16 for idealized step and top-hat wind inputs. Continuous plot is analytical solution, dashed line is model solution. Layer thicknesses (bottom panel) are those favourable to the enhancement of inertial frequency oscillations in the thermocline (Layer 2).

Figure 7. Figure of construction similar to Figure 6 showing cross-lake velocity components observed at three depths (Station 27: 10, 15, and 19m) (solid line), smoothed wind stress, and layer thickness from July 23 through August 15, 1979. On the figure are superimposed (dashed line) the corresponding outputs from the three layer numerical model.

Figure 8. Similar to Figure 7. but showing mid basin data and model output for the month of August, 1980.

A

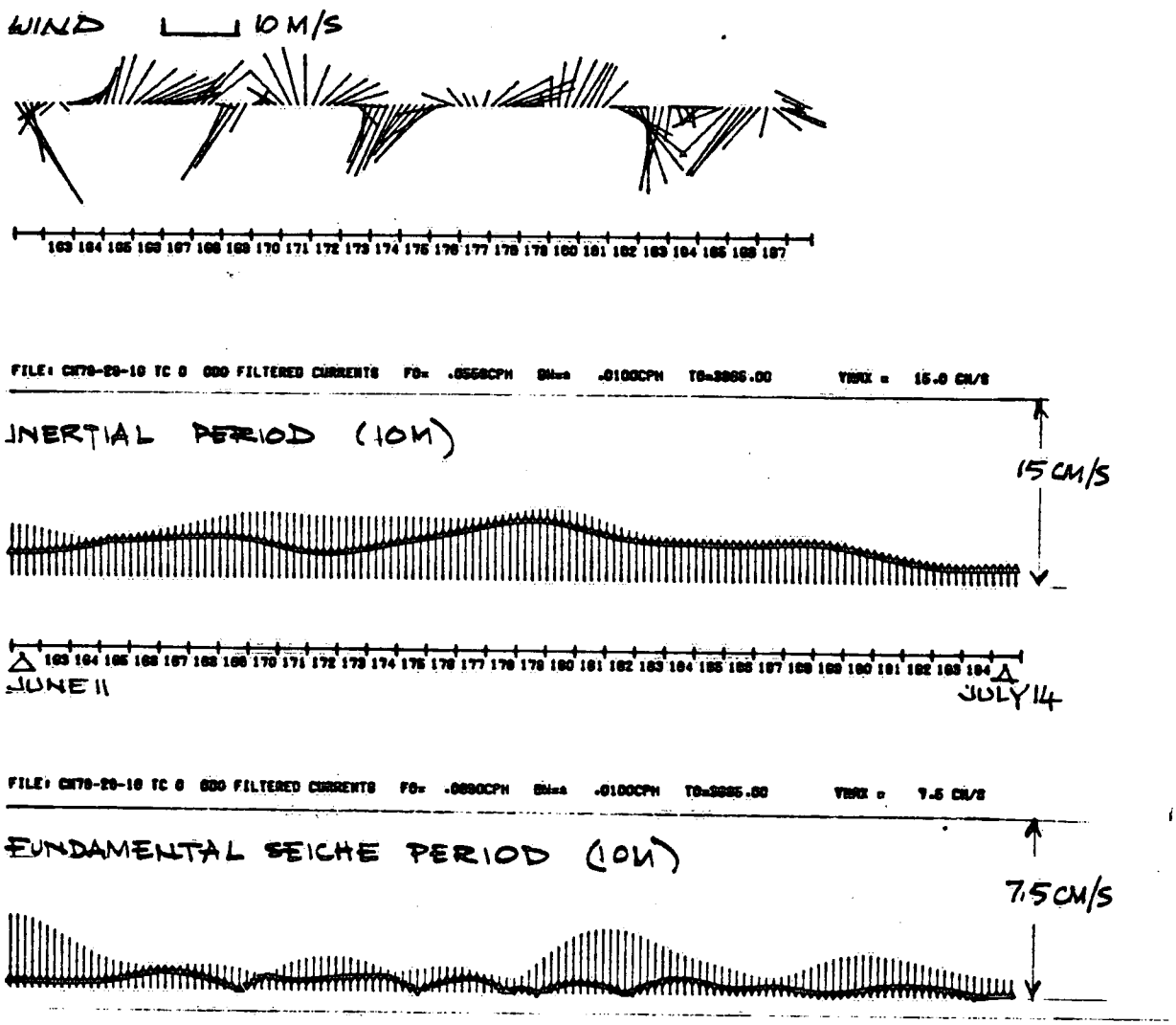
WIND
10 M/S
FILE: CM78-29-10 TC 0 000 FILTERED CURRENTS
INERTIAL PERIOD (10H)
15 CM/S
JUNE 11
JULY 14
FILE: CM78-29-10 TC 0 000 FILTERED CURRENTS
FUNDAMENTAL SEICHE PERIOD (10H)
7.5 CM/S

Figure 1A

B

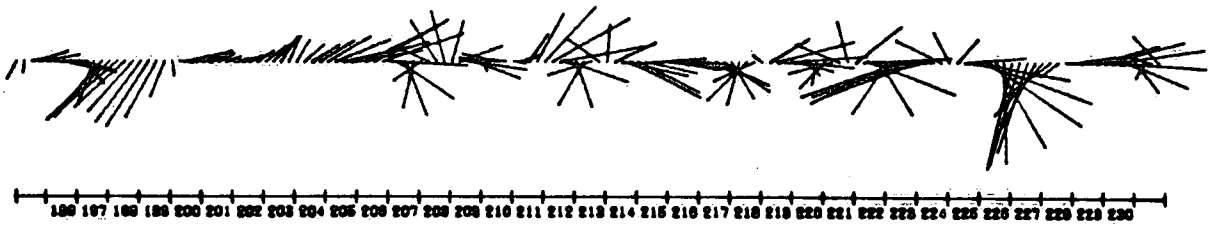

FILE: CM78-28-18 TC 0 600 FILTERED CURRENTS FB= .0050CPH Blco .0100CPH T0=4087.00 YMAX = 16.0 CM/S

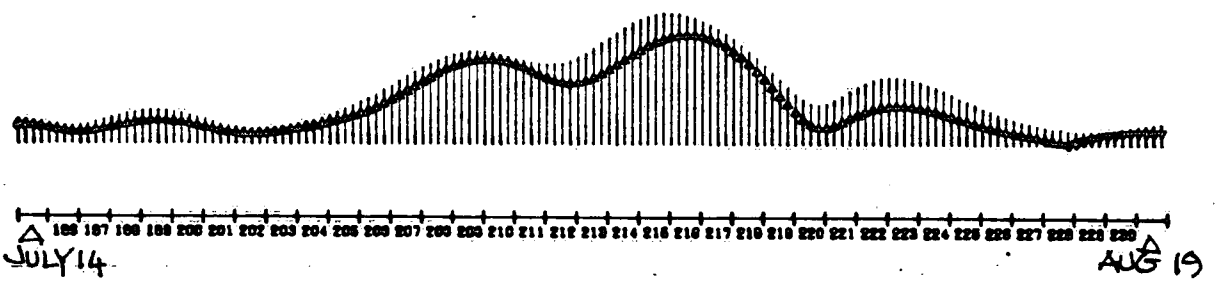

JULY 14 AUG 19

FILE: CM78-28-18 TC 0 600 FILTERED CURRENTS FB= .0050CPH Blco .0100CPH T0=4087.00 YMAX = 9.8 CM/S

Figure 4b

C

FILE: CM78-28-10 TC 0 000 FILTERED CURRENTS FO= .0558CPH BW=± .0100CPH T0=5401.00 YMAX = 15.0 CM/S

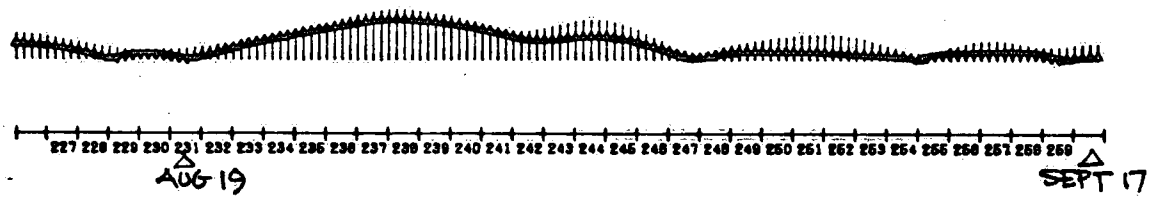

FILE: CM78-28-10 TC 0 000 FILTERED CURRENTS FO= .0690CPH BW=± .0100CPH T0=5401.00 YMAX = 7.5 CM/S

Figure 1 C

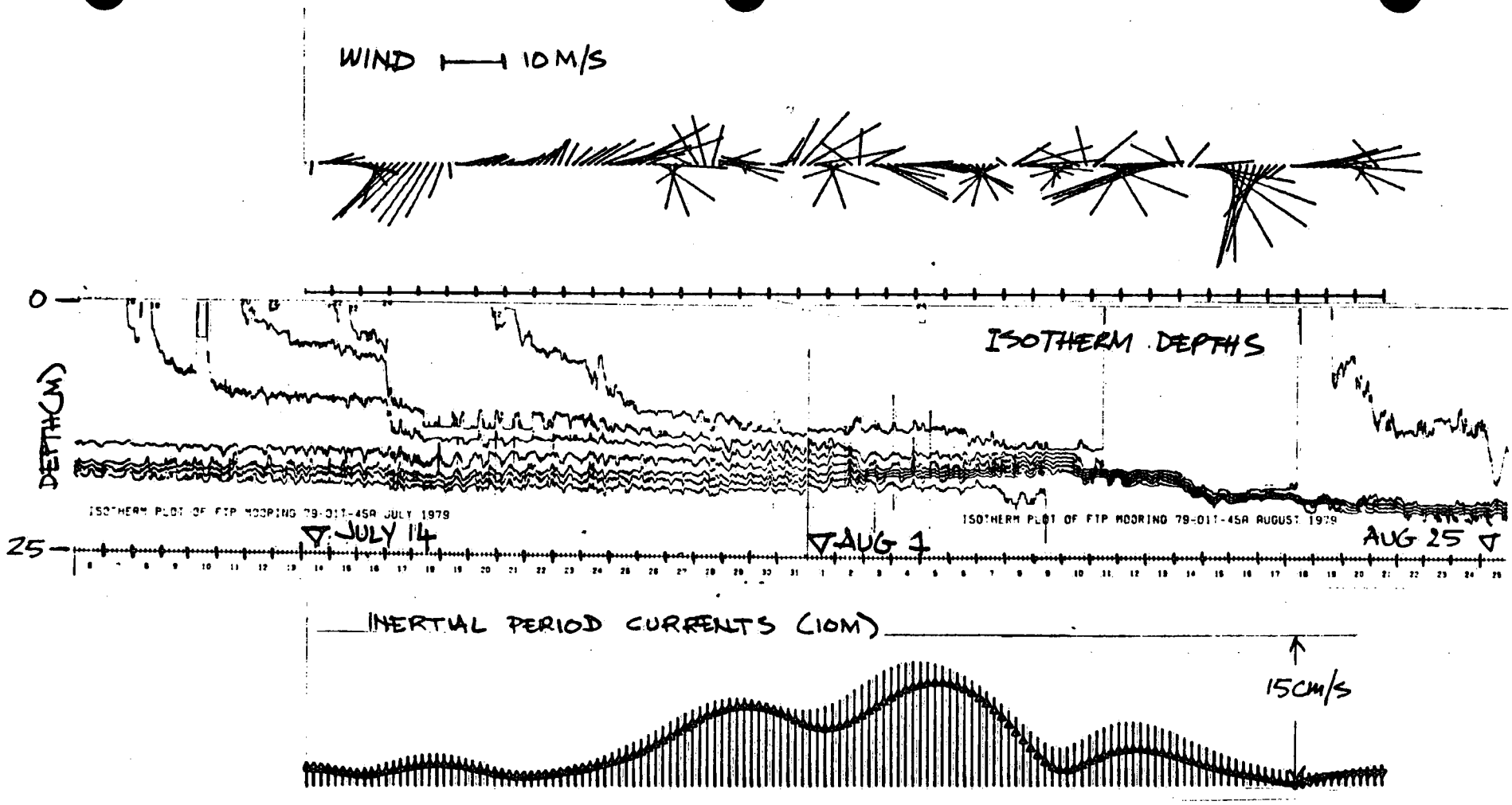

WIND, ISOTHERM DEPTHS, & INERTIAL PERIOD CURRENTS
MID-BASIN SITE JULY 14 - AUGUST 25, 1979

Figure 2

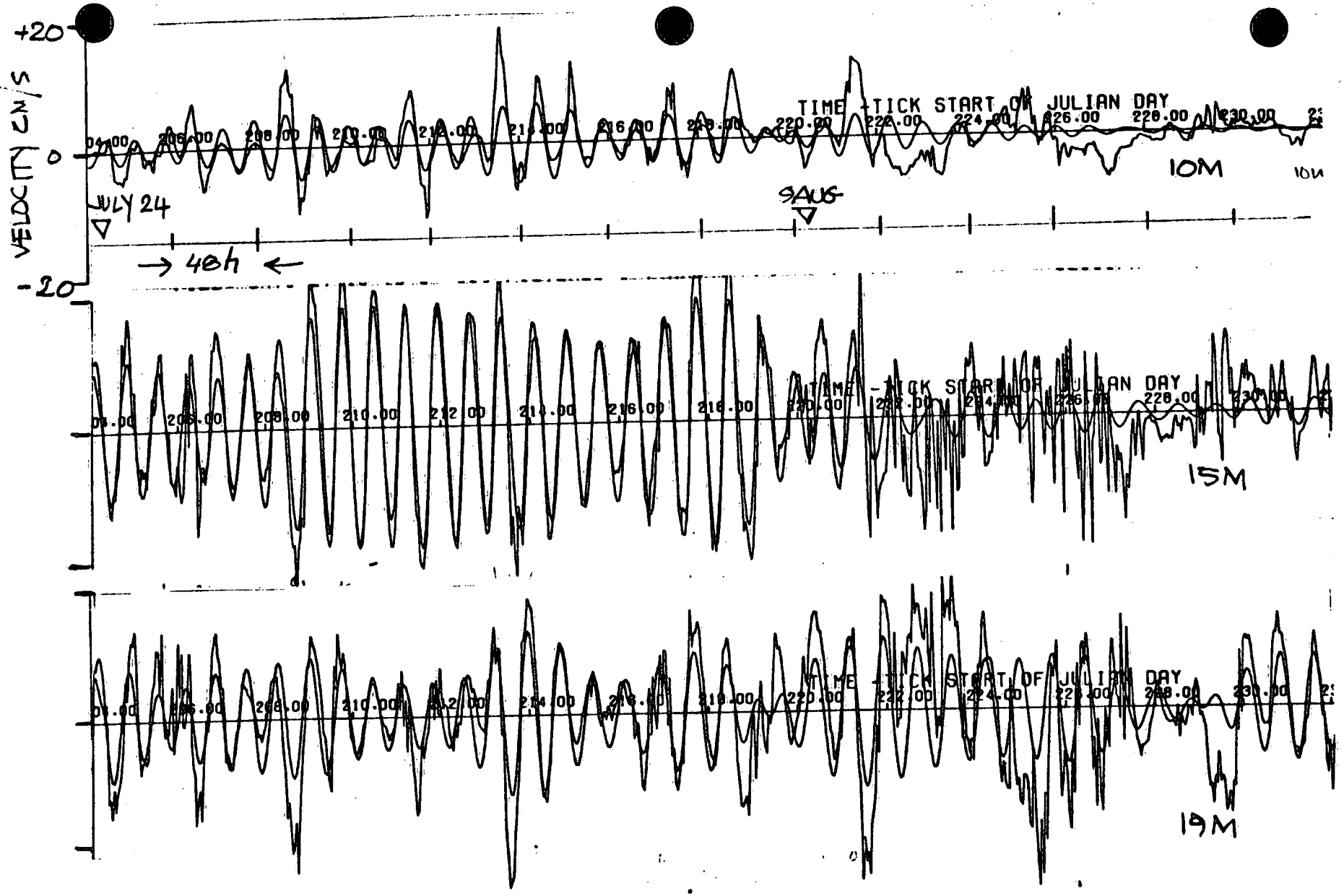

CROSS-LAKE COMPONENT OF CURRENTS STN 27 (MID BASIN) AT
10, 15, & 19M JULY 24 - AUG 20, 1979 FILTER 0.0558 ± .01 CPH

Figure 3

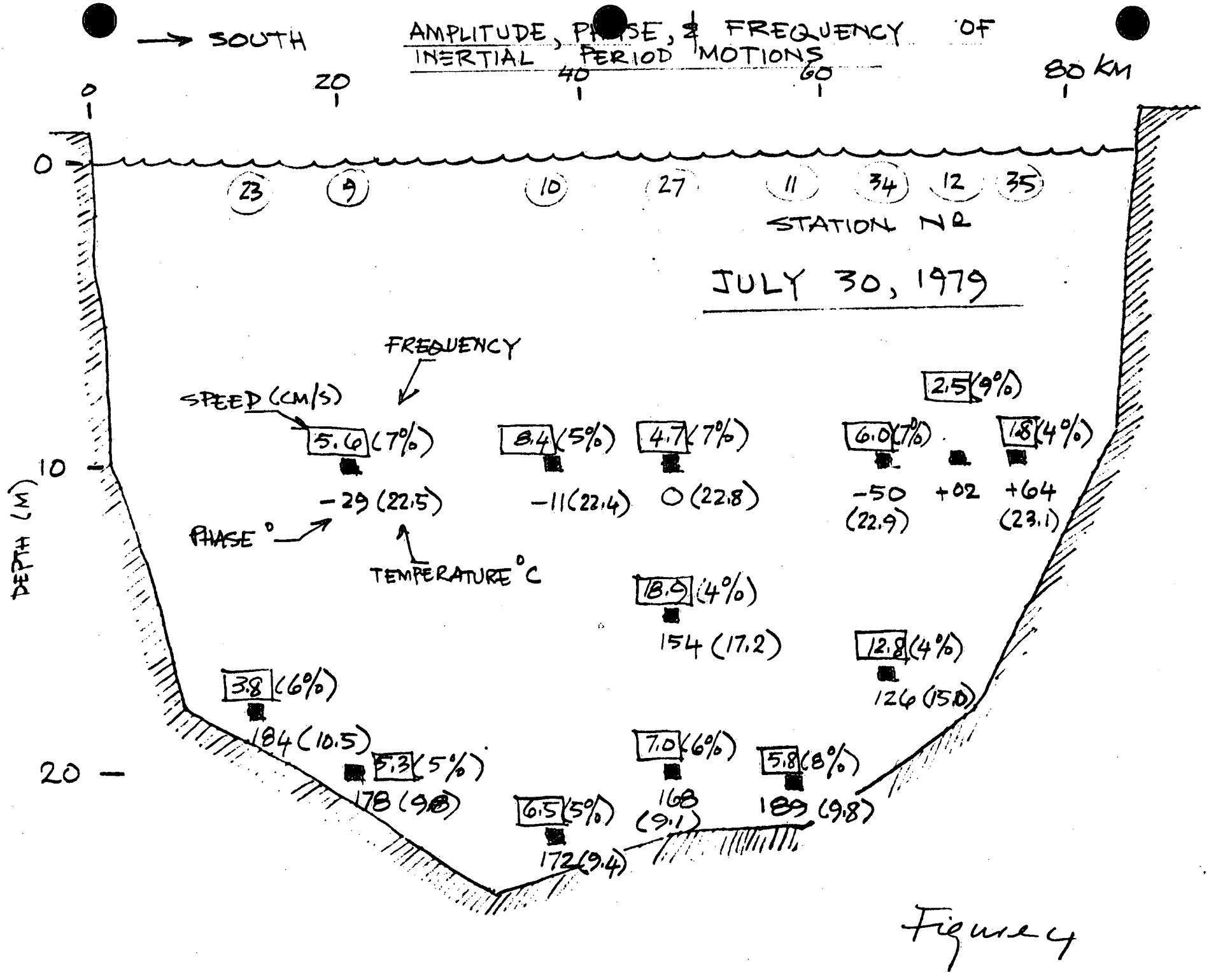
→ SOUTH
AMPLITUDE, PHASE, & FREQUENCY OF INERTIAL PERIOD MOTIONS
0
20
40
60
80 KM
0
10
20
DEPTH (M)
23
9
10
27
11
34
12
35
STATION NR
JULY 30, 1979
FREQUENCY
SPEED (CM/S)
5.6 (7%)
-29 (22.5)
PHASE °
TEMPERATURE °C
8.4 (5%)
-11 (22.4)
4.7 (7%)
0 (22.8)
2.5 (9%)
6.0 (7%)
-50 (22.9)
+02
1.8 (4%)
+64 (23.1)
18.9 (4%)
154 (17.2)
12.8 (4%)
126 (15.0)
3.8 (6%)
184 (10.5)
5.3 (5%)
178 (9.8)
6.5 (5%)
172 (9.4)
7.0 (6%)
168 (9.1)
5.8 (8%)
189 (9.8)

Figure 4

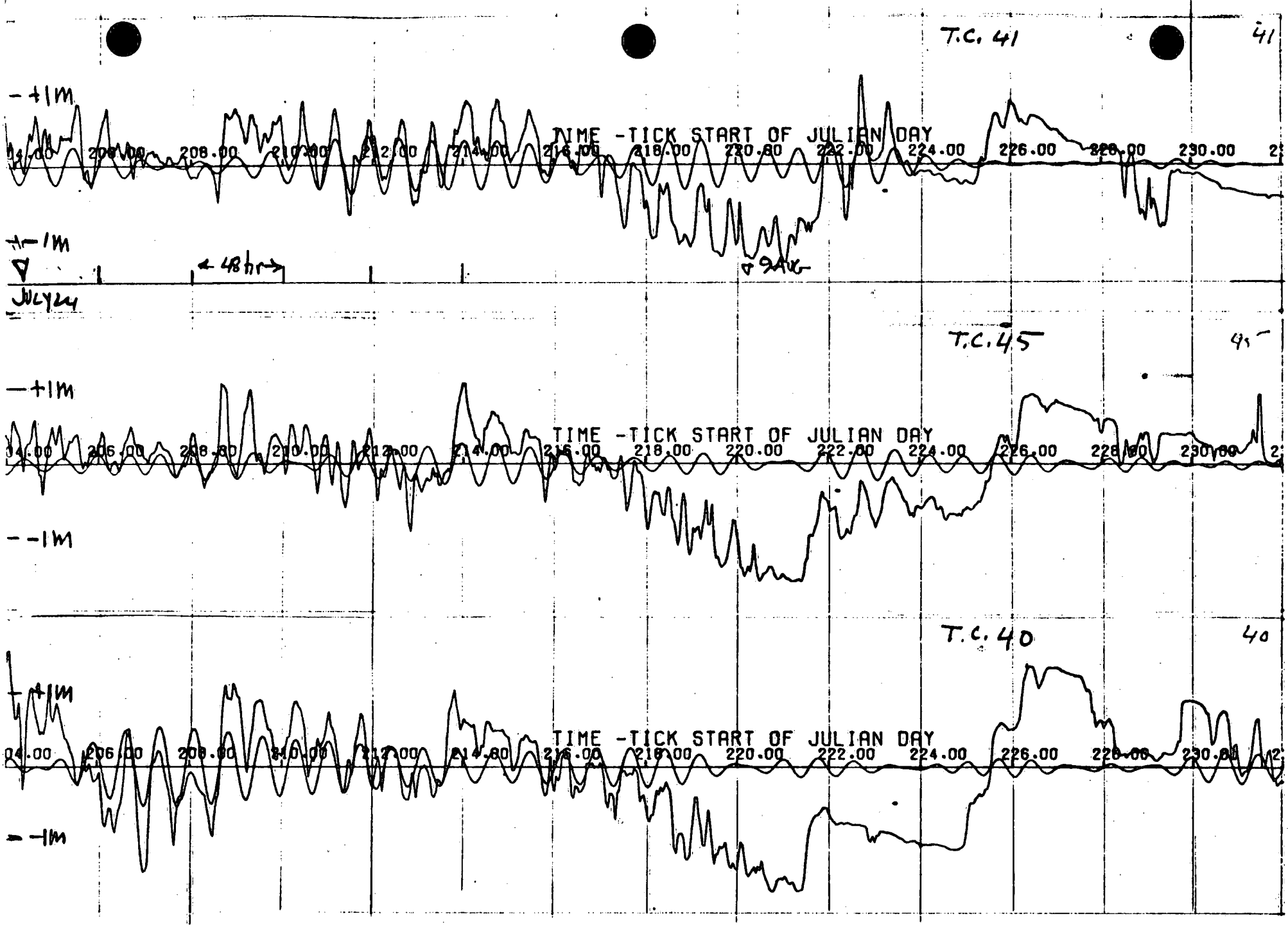
T.C. 41
41
+1M
TIME -TICK START OF JULIAN DAY
-1M
48hr
JULY24
T.C. 45
45
+1M
TIME -TICK START OF JULIAN DAY
-1M
T.C. 40
40
+1M
TIME -TICK START OF JULIAN DAY
-1M

Figure 5

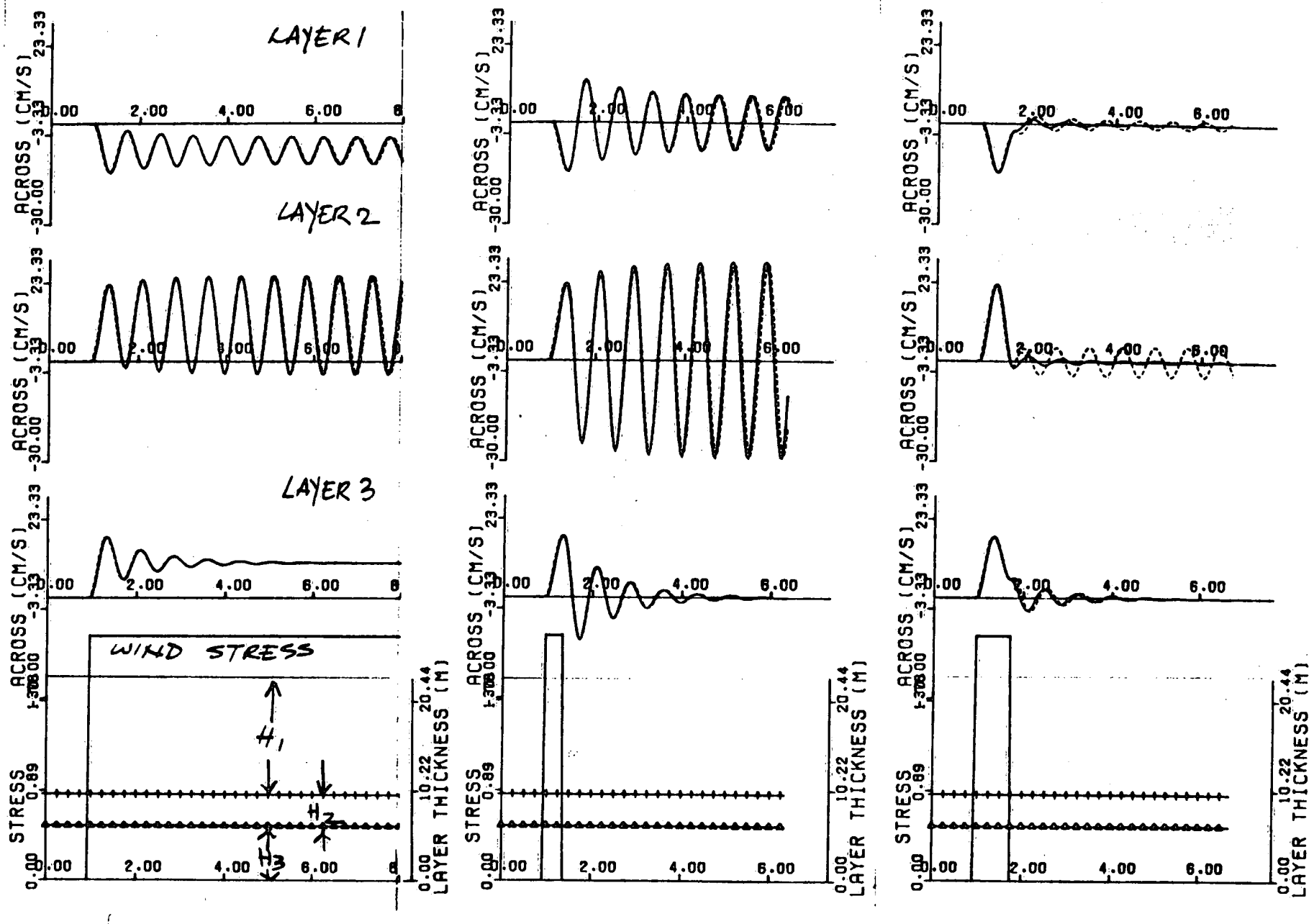

MODEL OUT PUT FOR IDEALIZED WIND INPUT AND CONSTANT LAYER THICKNESSES

Figure 6

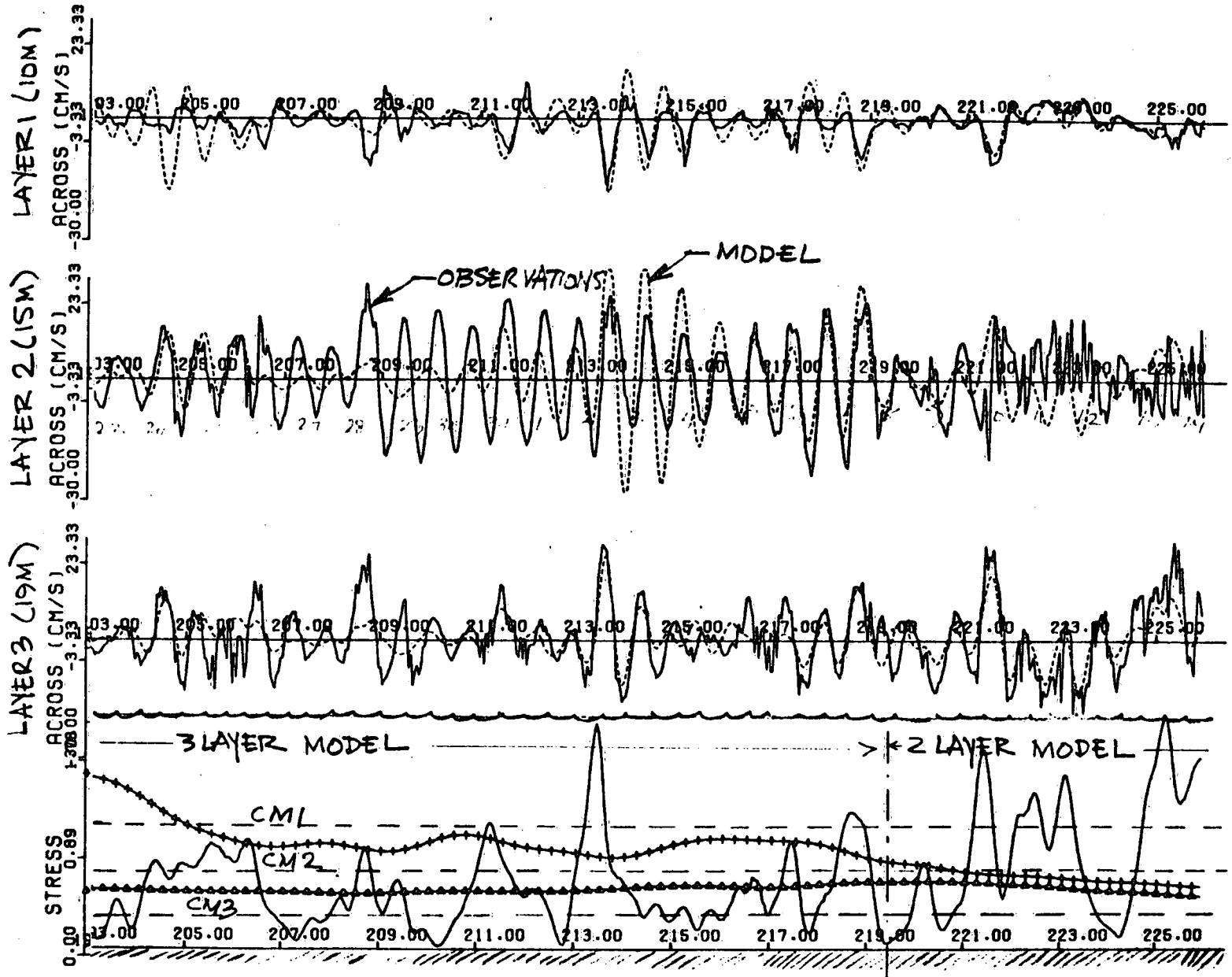

MODEL INPUTS & OUTPUTS JULY 23 - 15 AUGUST, 1979

Figure 7

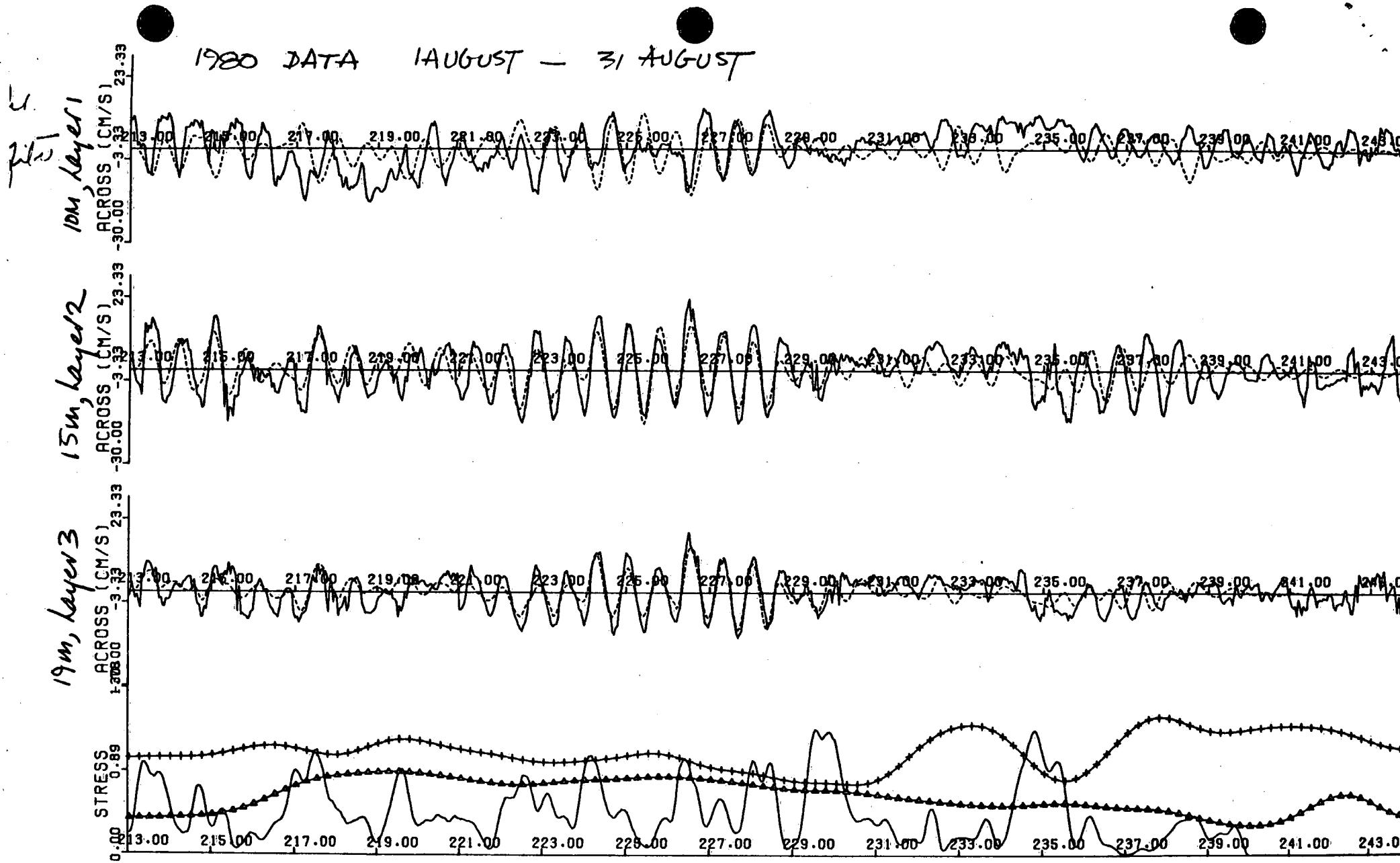
1980 DATA 1 AUGUST — 31 AUGUST
10m, layer 1
15m, layer 2
19m, layer 3
ACROSS (CM/S)
23.33
-3.33
-30.00
STRESS
0.89
0.00
213.00
215.00
217.00
219.00
221.00
223.00
225.00
227.00
229.00
231.00
233.00
235.00
237.00
239.00
241.00
243.0

Figure 8

Figure 9

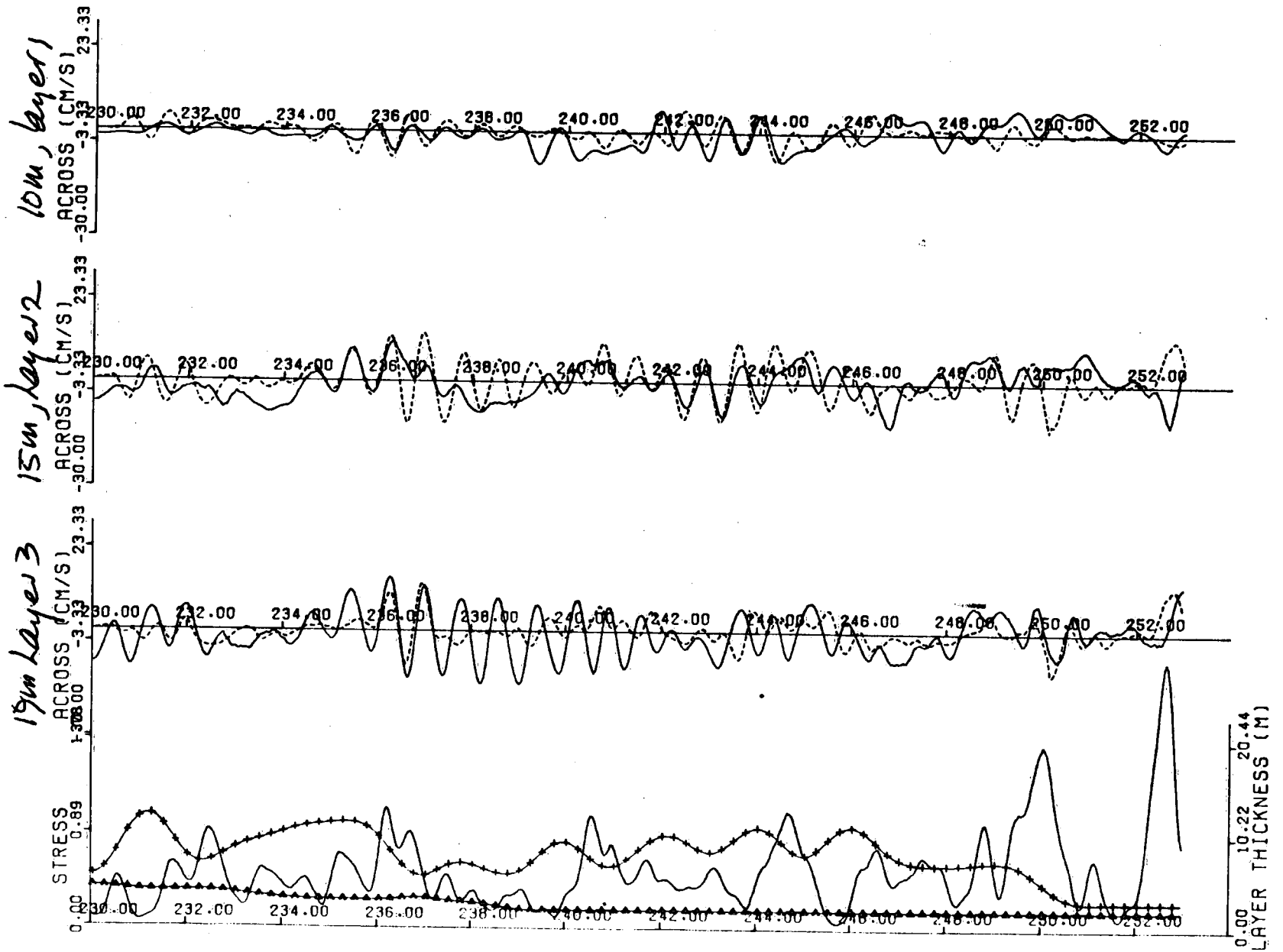
10m, layer1
15m, layer2
19m Layer 3
ACROSS (CM/S)
23.33
-3.33
-30.00
230.00
232.00
234.00
236.00
238.00
240.00
242.00
244.00
246.00
248.00
250.00
252.00
STRESS
0.89
0.00
LAYER THICKNESS (M)
10.22
20.44